Recent advances in the characterization and applications of biochar and hydrochar

Bruna Rijo[1], Ana Paula Soares Dias[1,2,*]

(1. *VALORIZA—Research Centre for Endogenous Resource Valorization*, *Polytechnic Institute of Portalegre*, 7300-555, *Portalegre*, *Portugal*;
2. *CERENA*, *Institute Superior Técnico*, *University de Lisboa*, 1049-001, *Lisbon*, *Portugal*)

Abstract: The conversion of biomass into carbon-rich materials, biochar and hydrochar, has emerged as a promising strategy to solve pressing environmental challenges while supporting sustainable industrial development. A comprehensive analysis of recent advances in the characterization and application of these materials, is provided, emphasizing their distinct production methods, physicochemical properties, and functional versatility. Biochar, typically obtained by pyrolysis at high temperatures, has a high porosity, aromaticity, and thermal stability, making it well-suited for applications such as CO_2 capture, electrochemical energy storage, catalysis, and soil improvement. In contrast, hydrochar, produced by hydrothermal carbonization in aqueous media at moderate temperatures, retains a higher number of surface functional groups and heteroatoms, offering advantages in aqueous-phase catalysis, pollutant adsorption, and bioremediation. The critical role of physicochemical characterization in optimizing material performance is outlined, and analytical techniques including liquid nitrogen adsorption, scanning electron microscopy, X-ray diffraction, X-ray photoelectron spectroscopy, Raman spectroscopy, infrared spectroscopy, Boehm titration, and thermogravimetric analysis are discussed. These show how physical-chemical characteristics such as surface area, functional group chemistry, and degree of graphitization, govern the materials' suitability for specific applications. Emerging uses in waste water treatment, biofuel production, animal feed, and advanced oxidation processes are examined, alongside their relevance to multiple UN Sustainable Development Goals, particularly in climate action, clean energy, and responsible production. The materials are versatile and can be produced on a large scale. Their performance can be fine-tuned using different production and post-treatment processes, making them key enablers in the transition to a circular, carbon-conscious economy.

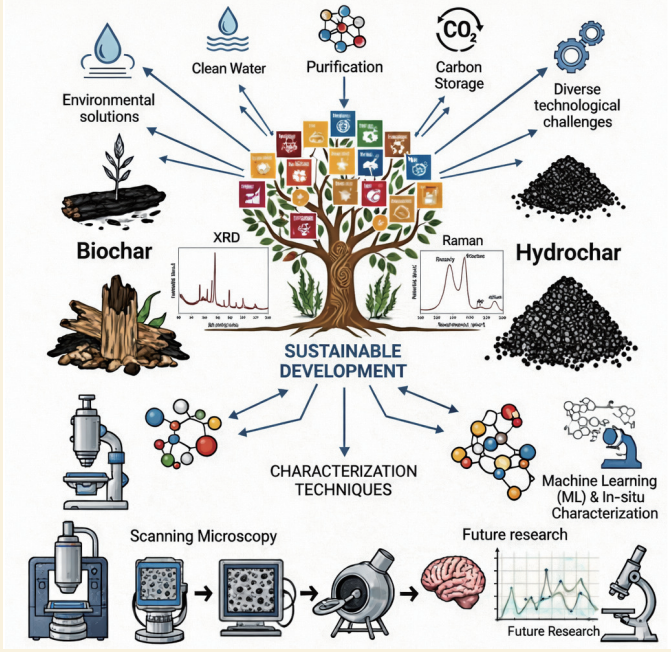

Key words: Biochar; Hydrochar; Characterization; Functional groups; Sustainable applications

1 Introduction

The innovative conversion of waste biomass (including agricultural, forestry, and industrial residues) into biochar and hydrochar creates versatile, carbon-rich materials with significant potential to address environmental concerns and enhance energy security. These materials are crucial for soil amendment, pollution remediation, carbon sequestration, and advanced applications like electrochemical energy storage and catalysis. This valorization process directly supports multiple United Nations Sustainable Development Goals (SDGs)[1−2] by promoting SDG 12 (Responsible Consumption) through waste utilization, contributing

Received: September 22, 2025
Revised: December 14, 2025
Accepted: December 15, 2025

to SDG 13 (Climate Action) by greenhouse gas reduction, and fostering a circular bioeconomy that aligns with SDG 7 (Clean Energy) and SDG 9 (Innovation). This multifaceted contribution positions biochar and hydrochar as pivotal components in the global pursuit of a more sustainable and resilient future.

Biochar and hydrochar are both derived from biomass, but differ significantly in their production processes, structure and functional properties[3]. Biochar is typically produced through pyrolysis under limited oxygen conditions at high temperatures (>400 °C), resulting in a highly aromatic, porous structure with a large specific surface area and well-developed micro- and mesoporosity. Hydrochar, on the other hand, is produced through hydrothermal carbonization (HTC) at lower temperatures (180–250 °C) in aqueous environments, leading to a more functionalized surface rich in oxygen-containing groups and often higher heteroatom content.

The performances of these high-carbon materials in diverse applications are strongly dependent on their physicochemical properties, necessitating comprehensive characterization using techniques that assess chemical composition, morphology, degree of graphitization, and thermal and structural stability. The global biochar market reflects the growing industry and research interest in carbon-rich materials. The global biochar market is projected to grow significantly, from an estimated USD 877.15 million in 2024 to approximately USD 3111.96 million by 2034, demonstrating a robust compound annual growth rate (CAGR) of 13.5% over the decade[4]. This growth underscores the increasing relevance of biochar and hydrochar as multifunctional, sustainable materials that support both environmental resilience and industrial innovation.

This review summarizes recent advances in the characterization techniques applied to biochar and hydrochar and highlight the implications of the observed properties in emerging technological and environmental applications. The novelty of this review, which distinguishes it from previous literature, lies in its systematic, side-by-side comparison of hydrochar and biochar by structuring the discussion around how each physicochemical characterization technique reveals their distinct properties.

2 Applications

Biochar and hydrochar are carbon-rich materials[5] produced from biomass through different thermochemical pathways-pyrolysis or carbonization (slow pyrolysis) for biochar, and hydrothermal carbonization (HTC) for hydrochar. Due to the aqueous and lower-temperature conditions of HTC, hydrochar retains a higher oxygen content from the original biomass, resulting in a greater abundance of surface functional groups containing heteroatoms (e.g., O, N). In contrast, biochar undergoes more extensive devolatilization, releasing gaseous compounds including CO_2 and H_2O, which leads to a more porous structure with increased surface area but significantly fewer functional groups[6]. The distinct physicochemical properties of biochar and hydrochar make them suitable for a wide range of applications, often with complementary or specialized roles[7]. However, as illustrated in Fig. 1, both materials are most commonly applied in soil amendment, where their respective characteristics (such as porosity, nutrient retention, and surface functionality) can enhance soil health and productivity. Biochar has been used since ancient times to enhance and restore soil fertility, most notably in efforts to replicate the highly productive Terra Preta soils of the Amazon Basin[8]. These rich, dark soils were created by indigenous Amazonians who incorporated biochar and organic waste into the earth, significantly improving its agricultural potential. Similar practices were also employed in ancient China and Japan, where charred plant material and crop residues were used to enrich the soil. In parts of Africa, communities likewise amended soils with charcoal and organic matter to boost fertility. Carbon-rich soil additives offer numerous benefits for both soil health and plant growth, as summarized by Kozioł et al.[9] (Fig. 1).

Scientific research beginning in the 1950s confirmed that biochar improves soil quality by increasing water retention, enhancing nutrient availability,

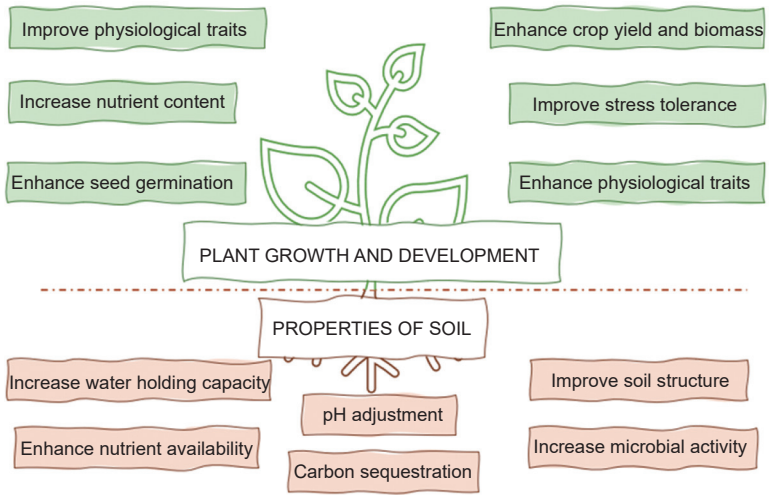

Fig. 1 Soil and plants improvements of biochar (Reproduced from[9])

stimulating microbial activity, and stabilizing pH levels. As a soil amendment, biochar reduces the need for chemical fertilizers and mitigates greenhouse gas emissions. It also contributes to long-term carbon sequestration while lowering methane and nitrous oxide release from soils[10]. In a recent review, Kozioł et al.[9] highlighted the multifunctional role of biochar, emphasizing its beneficial effects on soil health and plant growth (Fig. 1).

Wastewater treatment is one of the most relevant application fields for biochar and hydrochar (Fig. 2). Thanks to their morphological properties - notably the high specific surface area and porous structure, especially in the case of biochar - and the presence of surface functional groups containing heteroatoms (more pronounced in hydrochar), these carbonaceous materials can effectively remove various pollutants by adsorption[11]. These include heavy metals[12−13], dyes[14], pharmaceuticals[15] and personal care products[16], nutrients, organic contaminants[17], inorganic salts[18], pesticides[19], microplastics and nanoplastics[20]. In addition, biochar and hydrochar can serve as support media for microbial communities in bioreactors such as anaerobic digesters[21]. This enhances the biological degradation of organic matter and significantly reduces the amount of sludge produced.

The surface chemical composition of these chars - particularly those with alkaline characteristics - also enables they use as pH buffers in wastewater treatment processes[22]. This buffering capacity promotes biological process stability and improves overall treatment efficiency. Furthermore, biochar and hydrochar can be applied in advanced oxidation processes (AOPs) for the degradation of pollutants in wastewater[23]. These applications include persulfate activation[24], Fenton reactions and photocatalysis[25].

Other reactions of interest in the field of sustainable chemistry can be catalyzed by carbon-based materials[26]. Hydrochars rich in surface functional groups containing heteroatoms with acidic character, and further activated with sulfonic groups, have proven to be excellent catalysts for Fischer esterification reactions. Recently, Dias et al.[27] reported the production of methyl oleate esters (biodiesel) using sulfonated carbons obtained through hydrothermal carbonization of sugars with simultaneous sulfonation. Additional results from the same research group showed that biochars derived from materials such as banana peels and doped with alkali metals are active catalysts for

Fig. 2 Schematic diagram illustrating the removal of contaminants from wastewater

biodiesel production by transesterification of low-acidity waste cooking oils[28]. The availability of surface functional groups with acidic character in hydrochars is the key factor determining their effectiveness as catalysts in biodiesel production[29]. This factor also explains the distribution of biochar and hydrochar applications in the field of biofuel production (Fig. 2).

Biochar can be used as an additive in animal feed, improving digestion and gut health[30]. It helps balance the microbial population in the gastrointestinal tract, reducing harmful pathogens. In ruminant animals, biochar also contributes to lower methane emissions by altering fermentation processes, thereby enhancing the sustainability of animal protein production for human consumption (Fig. 3)[30]. Additionally, biochar has a detoxifying effect due to its high specific surface area and porosity, which allow it to adsorb toxins and heavy metals that may be present in contaminated feed. Biochar can be included in the diets of animals such as pigs, cattle and goats, at inclusion rates of up to 1% of the daily feed intake.

Biochar and hydrochar have recently emerged as low-cost sorbents for CO_2 capture but they differ significantly in performance (Table 1)[31].

Biochar generally exhibits a higher specific surface area and a more porous morphology, especially in materials that have undergone physical or chemical activation, resulting in a greater CO_2 adsorption capacity compared to hydrochar. Their main advantages lie in their sustainability, as they are derived from biomass, and in their tunable properties. The efficiency of CO_2 removal is influenced by characteristics such as

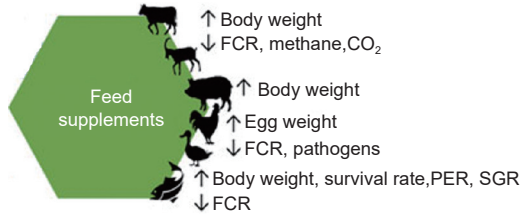

Fig. 3 Beneficial effects of using biochar as a feed additive on livestock farms (SGR- specific growth rate; PER- protein efficiency ratio; FCR - Feed conversion ratio. (Reproduced from[30])

specific surface area, pore distribution, and the presence of surface functional groups containing heteroatoms generally with acidic character. These features can be optimized through physical and chemical[34] activation processes. Optimized sorbents can achieve CO_2 adsorption capacities of up to 9 mmol/g, while maintaining excellent regenerability and stability over multiple adsorption–desorption cycles. The CO_2 adsorption mechanisms involve both physical and chemical interactions. The surface basicity of biochar enhances its ability to adsorb acidic pollutant gases such as SO_2 and NO_x, in addition to CO_2[35]. Studies highlight synergistic effects when biochar is combined with liquid-phase CO_2 absorbents, such as amines[35]. Overall, biochar and hydrochar are considered scalable and sustainable materials for CO_2 capture[36]. Ongoing research is focused on enhancing their physicochemical properties to enable industrial-scale deployment, thereby contributing to climate change mitigation[34].

Recently, carbonaceous materials derived from biomass have gained significant attention for their application in electrochemical systems[37], including supercapacitors, rechargeable batteries, and microbial fuel cells. Among these materials, biochar, a porous

Table 1 Comparison of CO_2 adsorption behavior of biochar and hydrochar (data collected from literature: morphologic characteristics and stability[32]; activation processes and CO_2 adsorption capacities[33])

Property	Biochar	Hydrochar
Surface area	High (up to 500–1500 m^2/g after activation)	Low to moderate (<100 m^2/g typically)
Porosity	Well-developed micropores and mesopores	Poorly developed porosity, mainly mesopores
CO_2 adsorption capacity	High (up to 3–5 mmol/g for activated biochar)	Lower (typically <1–2 mmol/g, unless modified)
Adsorption mechanism	Primarily physisorption via micropores; enhanced by N-doping	Primarily chemisorption via oxygen-containing functional groups
pH and surface chemistry	Often alkaline; fewer surface acidic groups unless oxidized	Acidic; rich in carboxyl, hydroxyl, carbonyl groups
Thermal stability	High – suitable for long-term CO_2 sequestration	Lower – prone to degradation under heat
Modification potential	High – effective activation (KOH, CO_2, steam), N-doping	Moderate – mainly surface functionalization
Best application phase	Gas-phase CO_2 capture	Aqueous-phase CO_2 interactions, precursor to advanced adsorbents
Environmental stability	Very stable (aromatic, graphitic structures)	Less stable (amorphous, aliphatic structures)

carbon-rich substance produced via pyrolysis of biomass, has emerged as a promising candidate due to its low cost, high specific surface area, and tunable surface functionalities. In supercapacitors, biochar serves as an electrode material capable of rapid charge/discharge cycles. Its performance is further enhanced through heteroatom doping (e.g., with N, S or P), which improves both electrical conductivity and capacitance due to pseudocapacitive effects and enhanced wettability[38–40]. In battery applications, such as Li-ion, Na-ion[41], and Li–S batteries[42], biochar is utilized as an anode material, offering high energy storage capacity and structural stability[42]. Composite materials combining biochar with transition metal oxides (e.g., Mn_3O_4–biochar) have shown to improve electrochemical stability and cyclability over prolonged charge/discharge cycles[43]. In microbial fuel cells (MFCs), biochar enhances the development of electroactive biofilms and facilitates efficient electron transfer, thereby improving overall cell performance[44]. Furthermore, biochar has been investigated in electrochemical wastewater treatment systems, acting as a support for electrocatalysts, where it contributes to increased pollutant degradation rates and energy efficiency[45].

Carbon-rich materials derived from biomass, such as biochar and hydrochar, offer a wide range of applications, many of which support the broader goal of sustainability by valorizing renewable waste resources. The suitability of biochar and hydrochar for specific applications is closely linked to their distinct physicochemical properties. For instance, biochar is typically valued for its high specific surface area and well-developed pore structure, which is critical in adsorption and electrochemical applications. In contrast, hydrochar is often characterized by a higher abundance of surface functional groups and heteroatom content, making it particularly useful in catalysis and environmental remediation.

Carbon materials, in addition to hydrochar and biochar, are essential components in various energy storage devices due to their excellent electrical conductivity, low cost, chemical stability and customizable structure[46]. They are widely used in batteries, such as lithium-ion and sodium-ion, and supercapacitors. The most common carbon-based materials in energy storage are generally categorized based on their ability to become graphitized at high temperatures. These include graphite, which has a highly crystalline, layered structure and is the dominant anode material in commercial lithium-ion batteries[47]. Another category is soft carbon, which is an amorphous carbon that can be fully converted to graphite at very high temperatures. There is also hard carbon, an amorphous (non-graphitizable) carbon with a disordered structure, which is highly important for next-generation batteries like sodium-ion batteries[48–49].

Given these application-specific properties, comprehensive physicochemical characterization of biochar and hydrochar is essential. The following sections detail analytical methodologies used to characterize these materials, with an emphasis on the key features assessed by each technique and their relevance to functional performance.

3 Characterization techniques

Derived from biomass, biochars and hydrochars exhibit physicochemical properties and are cheap, positioning them as promising heterogeneous catalysts. Their catalytic performance is governed by several intrinsic characteristics (Table 1). The data in Table 1 clearly shows that biochar and hydrochar exhibit distinct physicochemical properties, which critically influence their suitability for diverse applications[50]. Among these, specific surface area is particularly critical, as catalytic reactions occur predominantly on the catalyst's surface. Additional influential factors include chemical composition, degree of graphitization, crystallinity, and thermal stability. The following subsections explore the primary characterization techniques employed to analyze these properties in biochars and hydrochars.

3.1 Structure by BET (N_2 adsorption) and SEM (Scanning Electron Microscopy)

Biochar is produced through the carbonization or pyrolysis of lignocellulosic biomass, such as wood,

agricultural residues, starch, or sugar-rich seaweed. During thermal degradation, the breakdown of biomass components releases volatile compounds, including water and organic gases[51−52]. As these volatiles escape, they leave behind a porous carbon structure. Higher pyrolysis temperatures intensify this process, driving off additional volatiles and promoting the formation of microporosity, which enhances the biochar's overall porosity and specific surface area (Fig. 4).

Muzyka et al.[53] investigated the impact of pyrolysis temperature, heating rate, and residence time on the morphological characteristics of wheat straw biochar. Nitrogen adsorption analysis revealed high BET surface areas, with microporosity (<2 nm; IUPAC classification[54]) as the dominant pore structure. As expected, higher pyrolysis temperatures positively influenced the specific surface area (Fig. 5). Additionally, while increasing residence time enhanced the BET surface area at lower pyrolysis temperatures, it had a diminishing effect at higher temperatures. Higher pyrolysis temperatures generally increase surface area up to a critical threshold (600–700 °C), beyond which pore collapse may occur[55]. For example, Handiso et al.[56] investigated pine wood biochar and reported BET surface areas of 1.2 m^2/g for carbonization at 300 °C (producing a macroporous structure) and 393 m^2/g for carbonization at 500 °C (resulting in a microporous material). This demonstrates that elevated temperatures enhance porosity development until structural degradation limits further gains. Table 2 shows the main physical-chemical characteristics of biochar and hydrochar catalysts.

In lignocellulosic biomass-derived biochar, the specific surface area exhibits a positive correlation with carbonization temperature. This relationship arises from the progressive condensation of lignin aromatic rings at elevated temperatures, accompanied by the rapid release of hydrogen (H_2) and methane (CH_4) gases during secondary decomposition processes[58].

The specific surface area of biochars, as reported extensively in the literature, varies significantly depending on the carbonized feedstock. Table 3 and 4 highlight this variability across diverse biomasses, with values rivaling those of zeolitic catalysts, demonstrating their potential as high-performance alternatives. The high inorganic content of raw biomass (such as ash-rich rice husks[59]) promotes an increased surface area of biochar, as these inorganic compounds act

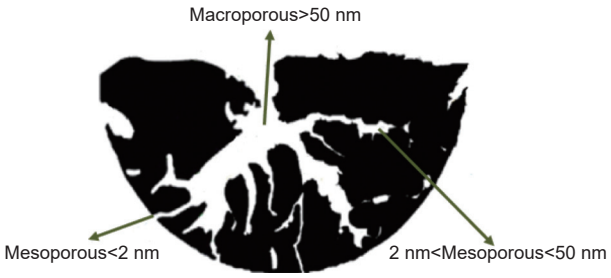

Fig. 4 Schematic representation of the porous network structure of biochar (Reproduced from[57])

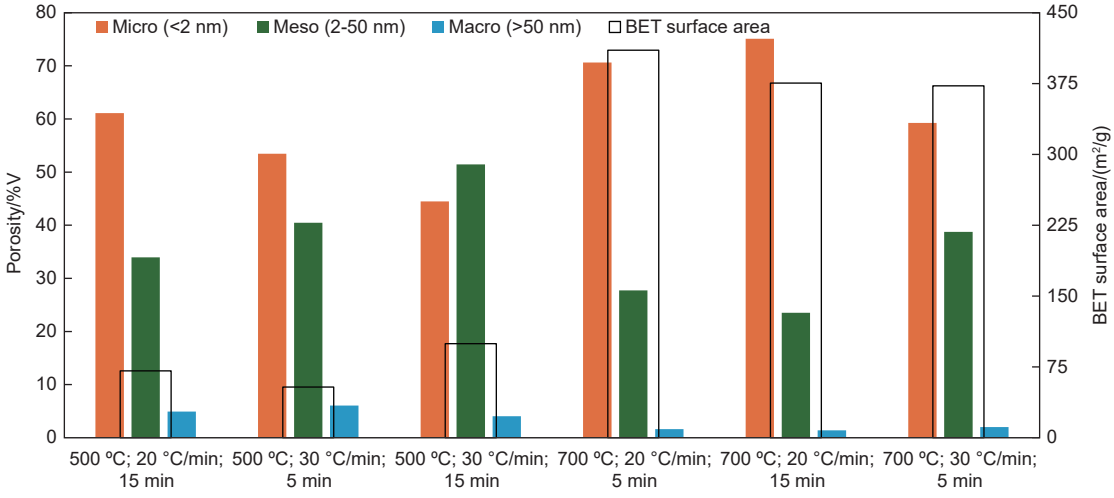

Fig. 5 Influence of pyrolysis temperature, heating rate, and residence time on the porosity distribution and BET surface area of wheat straw biochar (Reproduced from[53])

Table 2 Biochar versus hydrochar catalysts main physical-chemical characteristics

	Biochar	Hydrochar
Production method	Carbonization	Hydrothermal carbonization
Porosity	High	Low to moderate
Surface area	Large	Smaller
Oxygen content	Lower	Higher
Thermal stability	High	Moderate
Hydrophobicity	High	Low
Application	High-temperature	Liquid-phase catalysis

as volatilization catalysts during the biomass carbonization/pyrolysis process. On the other hand, sewage sludge produces biochar with a low surface area due to its high inorganic content (ashes)[60]. Biochar derived from sewage sludge (SS) is particularly significant due to the large quantities of this waste generated globally. Its valorization helps prevent improper disposal in landfills. The BET surface area of SS-derived biochar is influenced by the carbonization or pyrolysis conditions. According to the literature, increasing the heat treatment temperature generally enhances the surface area of the biochar, although it typically does not exceed 100 m^2/g and can be as low as 0.5 m^2/g[61].

Hydrochar is produced through the hydrothermal carbonization of biomass at moderate temperatures (180–250 °C) and autogenic pressure. This process promotes hydrolysis and condensation reactions. Compared to biochar, hydrochar typically has a lower specific surface area because it retains more oxygen from the original biomass, which reduces the release of volatile compounds responsible for pore formation. Thus, hydrochar has denser particles with lower porosity. Hydrochar consistently exhibits low microporosity, as its pores are typically filled with soluble organic compounds (tar) formed during hydrothermal carbonization. The dominant pores in the chars obtained by HTC are in the 1 to 20 μm range, i.e., macropores[62].

Scanning electron microscopy (SEM) allows for the evaluation of surface morphology for materials produced by either carbonization or hydrothermal carbonization. Biochar, a pyrolysis-derived material, is characterized by a very porous morphology clearly resolvable by SEM. With extensive literature available, a large database of SEM images exists, such as the micrographs in Fig. 6, which were obtained by Liu et al. for carbons from cereal straw processed between 300 and 700 °C[63].

Table 3 BET surface area of biochars prepared from several biomasses at different temperatures and heating rates

Biomass	Pyrolysis temperature/°C	Residence time	Heating rate /(°C/min)	BET surface area/(m^2/g)	Ref.	Notes
Pine wood waste	300-600	2 h	10	27-204	[64]	High carbon content, slow pyrolysis.
Rice husks	300-700	3 h	15	78-378	[59]	High silica content enhances porosity.
Corn stover	500-800	2 h	20	149–357	[65]	Moderate surface area, influenced by lignin.
Coconut shells	400-1000	2 h	5	130-702	[66]	Dense feedstock, high-temperature pyrolysis.
Sewage sludge	300-500	30 min	17	4-18	[60]	Low surface area due to ash content.
Switchgrass	550	1 h	10	200–250	[67]	Grass biomass with moderate porosity.
Bamboo	400-800	2 h	8	392-586	[68]	Fibrous structure enhances surface area.

Table 4 BET surface area of hydrochars prepared from several biomasses at different temperatures

Biomass	HTC temperature/°C	Residence time	BET surface area (m^2/g)	Ref.	Notes
Corn straw with 5% citric acid solution	190-250	3 h	5-14	[69]	The maximum BET surface area was reached at 220 °C
Rice straw with 5% citric acid solution	190-220	3 h	13-17		
Almond shell	220	20 h	4	[70]	The low surface area and porosity of HC can be attributed to pore blockage caused by residual volatile matter that was not transferred to the liquid phase during the HTC treatment, or by organic compounds from the liquid phase that migrated to the HC surface.
Palm shell	180-260	0.5-2 h	4-13	[71]	The increase in surface area was due to hydrogen bond breaking, phase change, or the breakdown of the palm shell's fibrous structure from reaction temperature and time, which created pores on the hydrochar surface.
Green waste	190	1 h	9-17	[72]	The surface area increased with microwave heating.

SEM images in the Fig. 7 reveal that as the carbonization temperature rises for the same biomass, the original morphological characteristics are lost due to intensified volatilization. This volatilization process is advantageous, as it directly promotes the formation of a more porous morphology. The optimization of biochar morphology hinges on controlling key factors, with lignocellulosic biomass being the preferable feedstock and a moderate pyrolysis temperature (400–700 °C)[73] being the most suitable condition. Furthermore, chemical activation is the most effective post-treatment for enhancing the final morphological and functional properties of the material[74]. The micrographs in Fig. 7 demonstrate that a post-pyrolysis treatment significantly boosts biochar porosity. The method involves first treating the biochar with strong bases (NaOH or KOH), then heat-treating it at high temperatures (>800 °C) with CO_2 as an oxidant. This two-step process removes less graphitized material, resulting in increased surface area and porosity.

The use of pyrolysis catalysts such as alkali carbonates in the production of biochar also acts as a

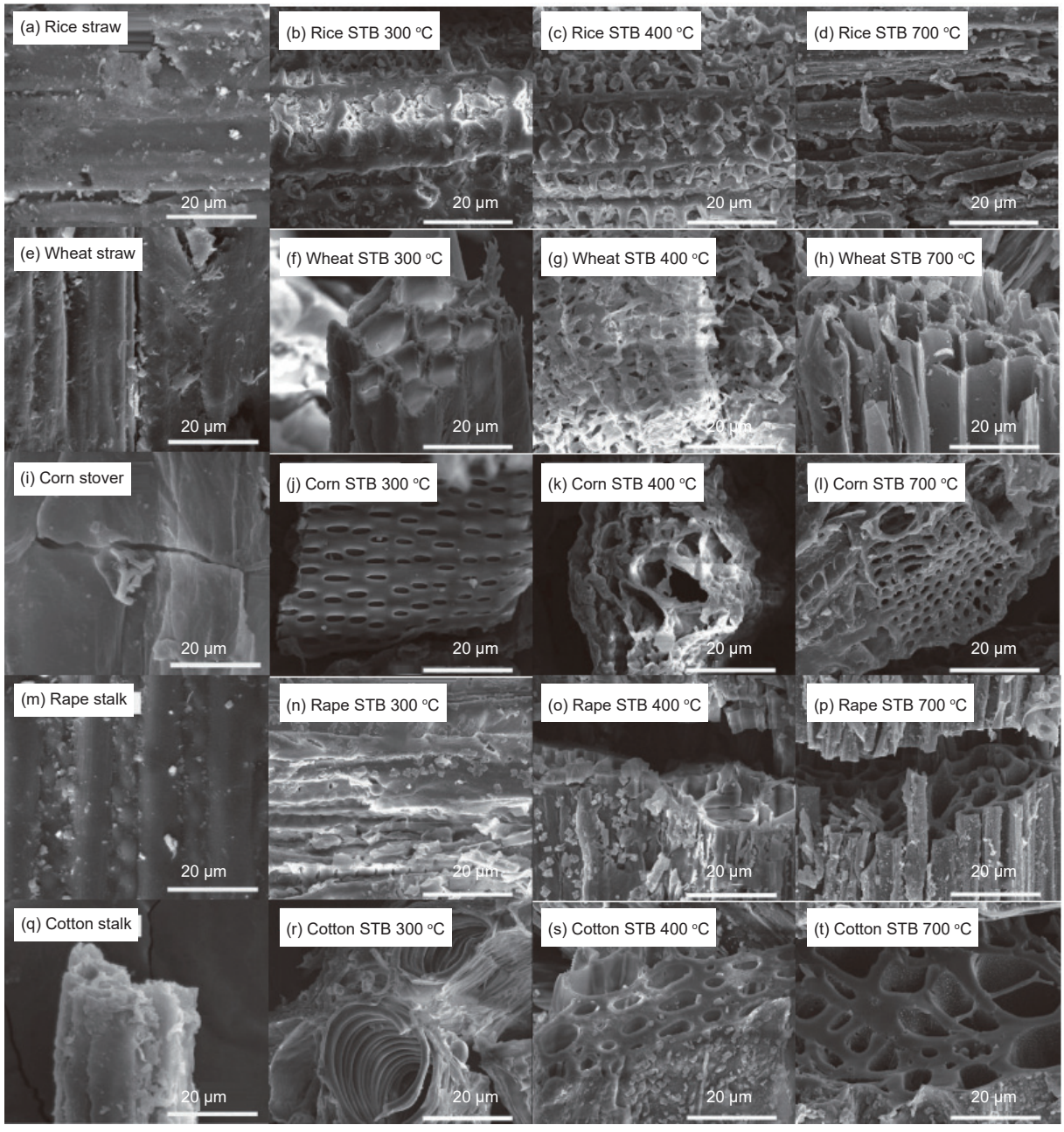

Fig. 6 SEM images of biochars obtained by carbonization of crops residues (Reprinted from[63])

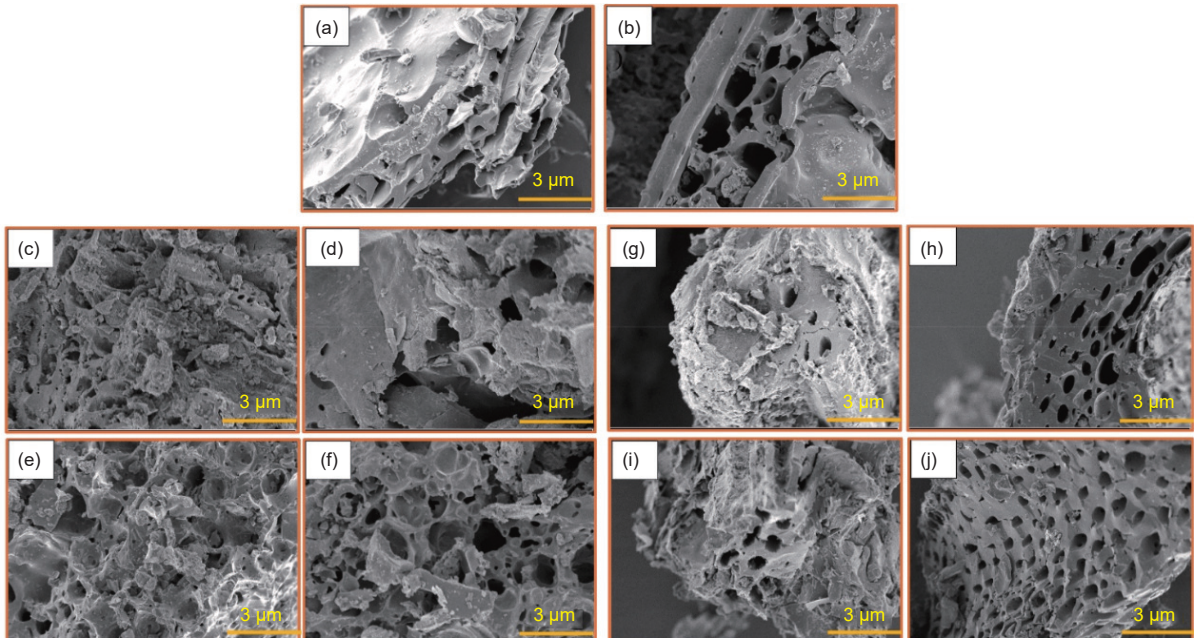

Fig. 7 Effect of chemical activation treatment on biochar morphology assessed by SEM: (a) Untreated BC (N_2). (b) Untreated BC (CO_2). (c) NaOH-BC (N_2). (d) NaOH-BC (CO_2). (e) KOH-BC (N_2). (f) KOH-BC (CO_2). (g) BC (N_2)-NaOH. (h) BC (CO_2)-NaOH. (i) BC (N_2)-KOH and (j) BC (CO_2)-KOH (Reproduced from[73])

porogen (Fig. 8), thereby obviating the need for a separate chemical activation step. Typically, these catalysts remain within the biochar matrix, which consequently increases its inherent basicity[28,75].

SEM images analysis consistently reveals that hydrochar possesses a porous and complex surface structure, a critical feature for applications like adsorption. The specific morphology is highly dependent on both the starting feedstock and the hydrothermal carbonization conditions, such as temperature. SEM images often depict a high degree of surface porosity, sometimes showing the hydrochar as spherical particles (Fig. 9)[76], which may be fused together, or as a multilayered carbon structure with an intricate network of pores.

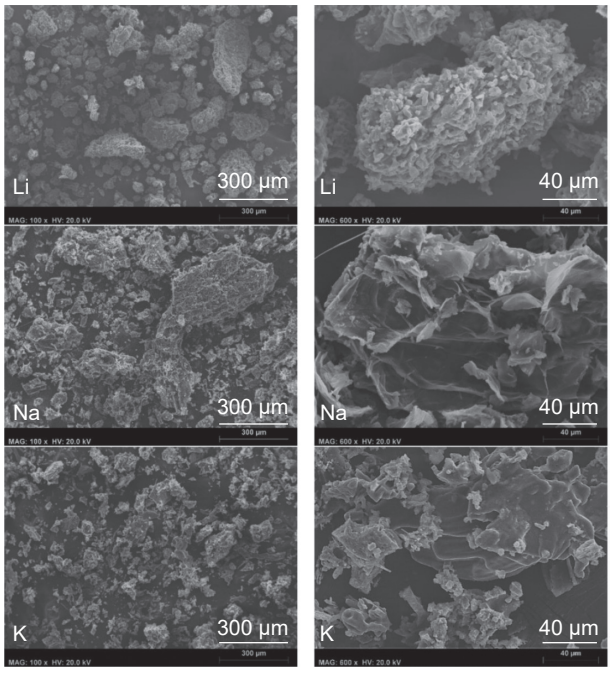

Fig. 8 SEM images of biochars obtained by catalyzed pyrolysis (low temperature) of banana peel. Reproduced from[28]

According to the literature $ZnCl_2$ is a prominent chemical activation agent used to synthesize porous carbon materials from biomass, serving as a Lewis acid and dehydration agent[77]. Despite the activation, this effect is not visible in the micrograph of the $ZnCl_2$-activated sample; instead, there appears to be a reduction in the size of the spheres.

Non spherical and low porosity morphology was observed by Spataru et al.[78] and Souza et al.[79]. for hydrochar derived from sugars and sugar alcohols obtained by simultaneous HTC and sulphonation at room pressure (Fig. 10).

3.2 Elemental composition

The comparison between biochar and hydrochar is generally carried out by evaluating key characteristics such as elemental composition, specifically the contents of carbon, hydrogen, nitrogen, sulfur, and

oxygen through ultimate analysis. Furthermore, the contents of carbon, hydrogen, and oxygen are utilized to construct a Van Krevelen diagram. This diagram (Fig. 11), which plots the H/C ratio against the O/C ratio, highlights the main characteristics of the chars and allows their comparison with natural substances like biomass, peat, lignite, coal, anthracite and others[80−81].

Elemental analysis provides insights into the changes in carbon content and helps clarify the reaction mechanisms through H/C and O/C ratios, which are key indicators of aromaticity and polarity. A lower H/C ratio signals increased aromaticity, whereas a higher O/C ratio suggests enhanced polarity[80−82]. A reduction in the H/C ratio as the peak temperature increased reflects the development of greater aromaticity and enhanced stability in both biochars and hydrochars formed at higher temperatures. When comparing the 2 thermochemical processes, biochars consistently exhibited lower H/C ratios than hydrochars, indicating that biochars possess a higher degree of aromaticity and structural stability[80−82]. It has been reported that the aromaticity increases along the sequence biochar > hydrochar > biomass, while polarity displays an inverse trend. This behavior is largely influenced by processing temperatures: pyrolysis at elevated temperatures leads to materials richer in carbon and poorer in functional groups, due to the release of O− and N−containing gases[80−82].

3.3 X-ray photoelectron spectroscopy (XPS)

XPS analysis of the biochar surface revealed

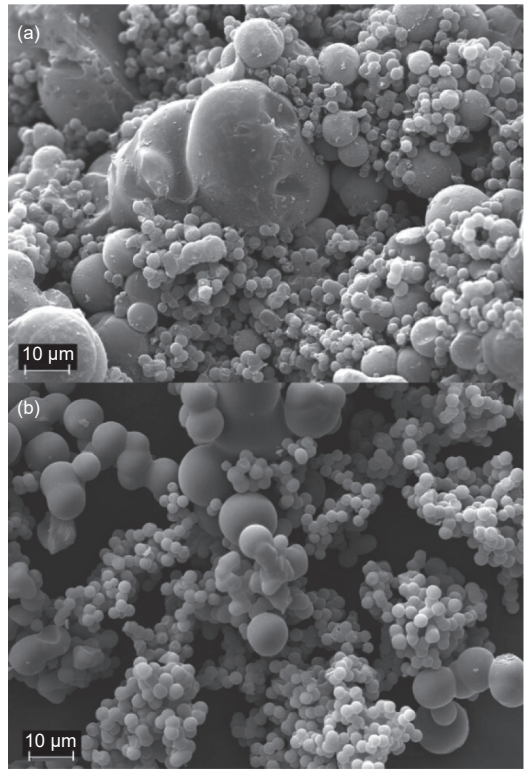

Fig. 9 SEM images of (a) hydrochar from sucrose prepared at 200 °C for 24 h, and (b) after activation with ZnCl at 700 °C (Reprinted from[76])

three main carbon species from the C 1s spectra: C−C/C=C (284.6 eV), C−OH/C−O−C (286.0 eV), and C=O (288.0 eV). The C−C/C=C peak was the most abundant, comprising 52.9% to 73.52% across samples. With increased pyrolysis temperature (200 to 250 °C over 360 min), the proportions of C−OH/C−O−C and C=O increased to 36.81% and 10.29%, respectively, indicating greater oxygen functionalization. O 1s spectra further confirmed the presence of oxygen-containing groups, with peaks at

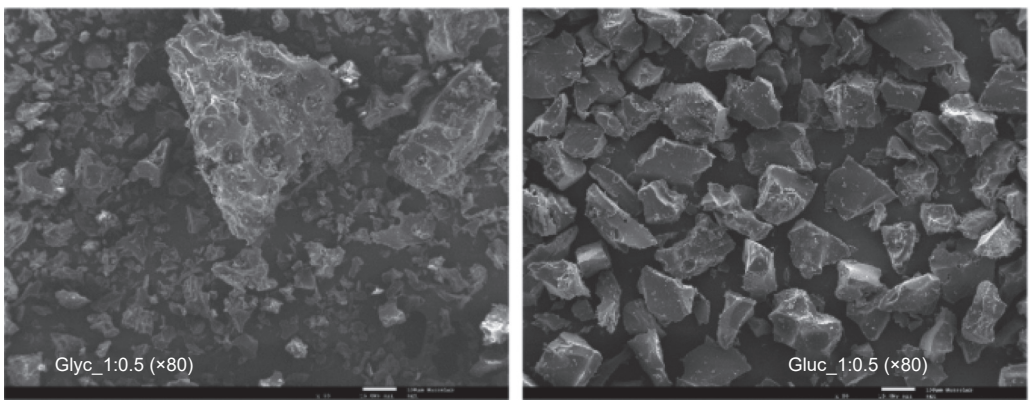

Fig. 10 SEM images of low non spherical and low porosity hydrochars from glycerin, and and glucose obtained at low pressure with simultaneous sulphonation (Reproduced from[78], copyright 2021, with Elsevier Permission)

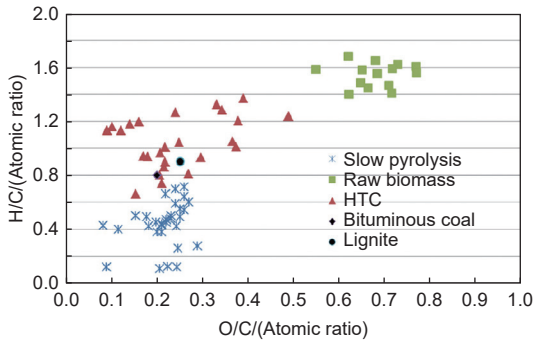

Fig. 11 Van Krevelen diagram illustrating the H/C and O/C atomic ratios of biomass, biochar and hydrochar. Lignite and bituminous coal are included as reference materials for comparison. (Reproduced from[5] copyright 2015, with Elsevier Permission)

531.0 eV (C=O) and 533.4 eV (C−OH/C−O−C). With the increase of temperature, the area of C−OH/C−O−C decreased (63.98% to 32.49%), while C=O increased (36.02% to 67.51%), suggesting dehydration reduced hydroxyl groups and increased carbonyl content, thereby lowering the O/C atomic ratio[83].

Li et al. studied the production of hydrochars from rice husk as adsorbents for removing organic contaminants using metal chloride-assisted hydrothermal carbonization[84]. The inclusion of metal chlorides (KCl and $CaCl_2$) in the feed solution enhances the process. XPS analysis of hydrochar samples revealed surfaces mainly composed of carbon (284.8 eV) and oxygen (531.8 eV), with minor amounts of nitrogen and silica. The C 1s spectra identified functional groups such as C−(C,H) (~ 284.5 eV), C−O (~ 286 eV), C=O or O−C−O (~ 287 eV), and COO− (~ 288.5 eV), indicating the presence of graphitic carbon and various oxygenated groups like hydroxyls, ethers, carboxyls and esters[84]. The distribution of these groups varies depending on the metal chlorides used during hydrothermal carbonization. Samples RHHK0.6 and RHHCa0.2 exhibited a decrease of C−(C/H) and C−O content but increased C=O/O−C−O and COO− levels, suggesting enhanced decomposition of rice husk components due to metal chloride addition, with $CaCl_2$ having a stronger effect than KCl. In contrast, RHHCa0.6 showed increased C−(C/H) and decreased oxygenated groups, indicating a more hydrophobic surface[84].

Yue et al. analyzed hydrochars produced from furfural residue residues using XPS. The C1s spectra revealed four main types of carbon bonds, including aliphatic/aromatic carbon groups (C−H, C−C/C=C, 284.7−285.0 eV), hydroxyl or ether groups (C−O, 286.1−286.7 eV), carbonyl groups (C=O, 287.7−287.9 eV), and carboxylic or ester groups (−COOR, 289.0 eV)[85]. As the temperature increased, the C−O bond intensity significantly decreased due to carbohydrate decomposition. Furthermore, the binding energies of C−C/C−H and C−O bonds shifted to higher values, indicating structural changes. This shift reflects the transformation of lignin-derived Ar−O−CH_3 (low binding energy) to cellulose-derived O−C−O structures (higher binding energy near 286.73 eV)[85].

3.4 X-Ray powder diffraction (XRD)

X-ray diffraction (XRD) is a powerful technique for characterizing carbonaceous materials produced through carbonization, pyrolysis, or hydrothermal carbonization. Fig. 12 shows a comparison of XRD patterns of bamboo biochar and hydrochar to emphasize the diffraction characteristics of carbonaceous materials produced by pyrolysis and HTC, typically observed as a diffraction feature around 2θ = 23°, along with less ordered structures appearing at 2θ = 43°. Generally, biochar produced by carbonization exhibits a higher degree of graphitization compared to hydrochar, which tends to have a lower carbon content and a more amorphous structure. The XRD peak at 23° is typically broad, indicating a high degree of structural disorder and the presence of small crystallites.

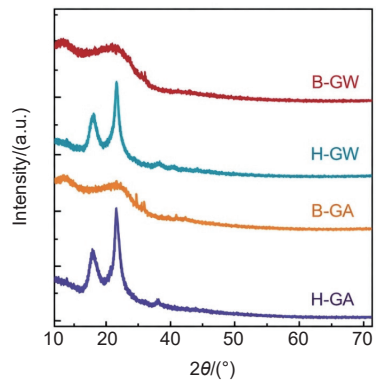

Fig. 12 XRD patterns of bamboo biochar and hydrochar Adapted from[86]

The diffractograms of biochar and hydrochar may also display additional lines, which are narrower than those of graphite and correspond to inorganic compounds such as calcite, sylvite, and quartz, among others. These minerals originate from the ash content of the biomass used as the raw material for biochar production. X-ray diffraction is therefore used to infer the composition of inorganics in the chars produced[87].

High-temperature thermal treatment (HTT) drives the structural transformation of biochar through a progressive ordering of its carbon matrix. Initially, there is an increase in disordered aromatic rings within the amorphous structure. As the temperature rises, these rings grow and rearrange into turbostratically aligned sheets of conjugated aromatic carbon. With continued heating, the structure becomes increasingly graphitic, developing order in the third dimension (Fig. 13[88]).

During HTT, hydrogen and heteroatoms (e.g., O) are released as gases, reducing the overall yield of biochar but resulting in a more condensed and ordered carbon structure. This transition reduces structural heterogeneity through 2 main processes: (1) the loss of amorphous material during gas evolution and (2) the transformation of disordered carbon into larger, more stable aromatic systems[88,89].

The XRD data of biochar (Fig. 14)[28], obtained by carbonizing banana peels at 350 °C, exhibit diffraction peaks corresponding to sylvite (KCl), which overlap with the broader, less crystalline diffraction pattern of the biochar. During the transesterification reaction, the leaching of the inorganic crystalline phase due to contact with methanol enhances the visibility of the expected biochar's diffraction pattern, revealing a prominent XRD feature centered at 23° and a weaker one at 43° which shows no significant difference from the simulated XRD pattern of biochar in Fig. 12.

Hydrothermal carbonization of banana peel catalyzed by H_2SO_4 produces a hydrochar with an XRD profile similar to that of biochar obtained by dry carbonization after ash removal (Fig. 15). During the

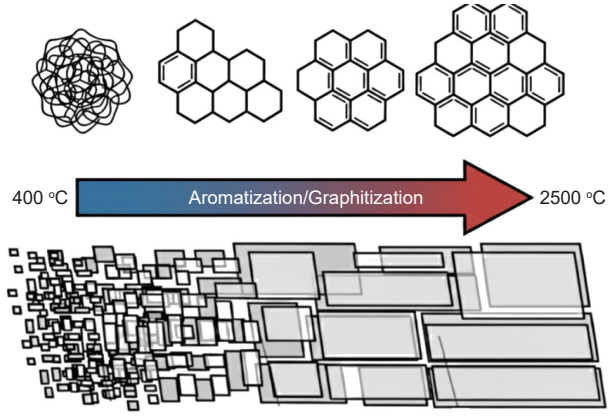

Fig. 13 Structural arrangement of carbon materials versus thermal treatment temperature. (Reproduced from[88])

HTC process, banana peel ash dissolves into the aliquots. Other sugar-based biomasses, such as sucrose, yield hydrochars with crystallinity comparable to that of banana peel. In contrast, orange peel subjected to HTC exhibits an XRD profile where the hydrochar's diffraction pattern overlaps with that of Ca-rich ash, which is converted to calcium sulfate due to sulfuric acid catalysis (Fig. 15). After catalyzing the esterification of oleic acid with methanol, the hydrochars show a noticeable reduction in the width of the XRD peak centered at 23°, suggesting partial removal of amorphous carbonaceous material through solubilization in the biodiesel produced.

Panwar et al.[90] investigated carbon materials obtained by pyrolyzing sugarcane bagasse and corncob - biomasses rich in cellulose and hemicellulose - using X-ray diffraction. The researchers observed a fading of the cellulose XRD feature in the 22°–23° range as

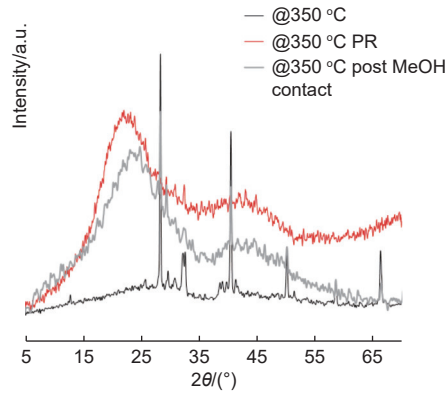

Fig. 14 XRD patterns of banana peel biochar obtained by carbonization at 350 °C raw and after leaching of inorganic sylvite phase in contact with methanol and post transesterification catalysis (Reprinted from[28])

the pyrolysis temperature increased from 500 to 700 °C. They attributed this to the formation of amorphous carbon materials, which exhibited a broad XRD pattern around 23°. They also noted that broader XRD features indicate more stable carbon materials. Sugarcane bagasse produced smaller crystallites than corncob, likely due to differences in ash content, which can act as a pyrolysis catalyst[91]. The narrow XRD peaks of the ash, in contrast to the broad peaks of the carbonaceous materials, were clearly visible in the XRD diffractograms of biochars derived from both biomasses.

3.5 Raman spectroscopy

Raman spectroscopy is widely used to assess the structural organization of carbonaceous materials[93]. The structural organization of biochar and hydrochar plays a fundamental role in their performance as catalysts or catalyst supports. Factors such as defect density and structural disorder enhance the number of available active sites, thereby increasing catalytic activity. Additionally, the presence of heteroatoms in functional groups can serve as adsorption centers for reactants, further enhancing their catalytic effectiveness. Such characteristics can be inferred from Raman spectra[94]. A typical Raman spectrum of a carbonaceous material, as shown in Fig. 16, exhibits 2 prominent bands: the *G* band at 1580 cm^{-1}, associated with graphitized material, and the *D* band at 1350 cm^{-1}, corresponding to disordered graphitized structures. The spectrum curve fitting reveals 3 additional, lower-intensity, bands (1620 (*D*2), 1500 (*D*3) and 1200 (*D*4); cm^{-1}), attributed to disordered graphitized material, inorganic impurities (~ 1200 cm^{-1}), and functional groups containing heteroatoms such as oxygen (1500 cm^{-1})[95]. The Valley band (~ 1500 cm^{-1}) is particularly relevant in hydrochar and biochar subjected to oxidative activation treatments. Guizani et al.[96] reported the existence of a correlation between the bands intensity ratio of *D*3/*D* and the (O+H)/C composition ratio of biochars obtained by pyrolysis for temperatures higher than 600 °C. Hydrochar and biochar exhibit distinct Raman signatures, allowing for clear differentiation (Fig. 17)[97].

The ratio of the intensities of the *D* and *G* bands, known as the graphitization index (I_D/I_G), serves as an indicator of structural order in carbon materials. Typically, materials synthesized by hydrothermal carbonization (HTC) exhibit a lower I_D/I_G ratio compared to their counterparts produced through carbonization or pyrolysis, indicating a higher degree of structural order[98]. The graphitization index of biochar or hydrochar catalysts is a key factor influencing their catalytic performance. Recently, Soares Dias et al.[27] reported that sugar-derived hydrochar catalysts with a higher graphitization index exhibit enhanced performance in the Fischer esterification reaction. This im-

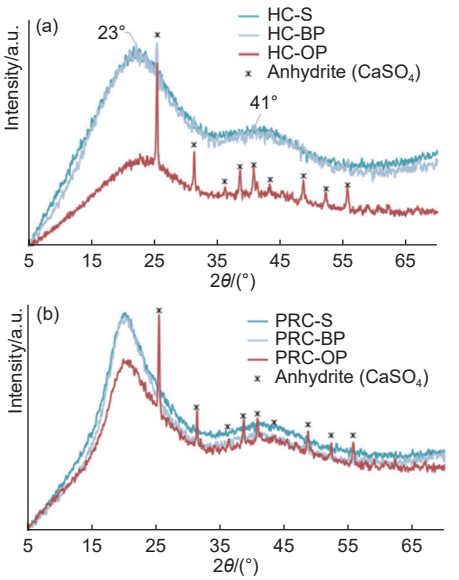

Fig. 15 XRD patterns of hydrochar produced by HTC catalyzed by H_2SO_4 as prepared (a) and post esterification of oleic acid with methanol (b) (HC-hydrochar; S- sucrose; BP-banana peel; OP-orange peel). (Reproduced from[92])

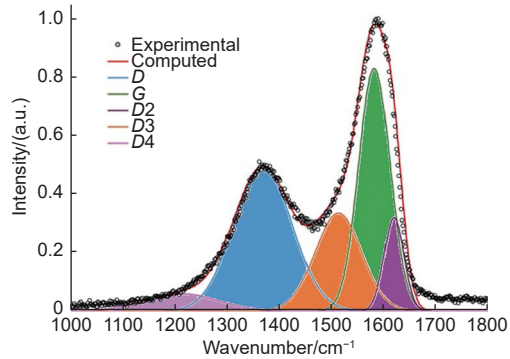

Fig. 16 Typical Raman spectrum, and fitted Raman bands[95], of a carbonaceous material obtained by hydrothermal carbonization of glucose catalyzed by H_2SO_4 (Reproduced from[27])

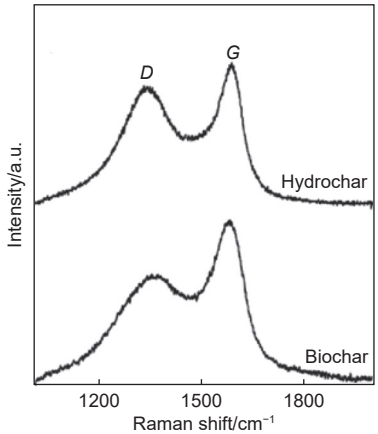

Fig. 17 Raman spectra of hydrochar (250 °C) and biochar (800 °C) from cellulose (Reproduced from[29])

provement is attributed to increased hydrophobicity, which rises with graphitization. Greater hydrophobicity makes the catalysts less sensitive to water, a byproduct of the esterification process, thereby enhancing their efficiency.

In contrast to the findings of Dias et al.[27], Clohessy and Kwapinski[99] reported higher catalytic activity in catalysts prepared through post-carbonization sulfonation for less graphitized materials. According to them sulfonation is more effective in materials with lower degrees of graphitization.

Markova et al.[100] also reported that less carbonized - and therefore less graphitized - materials exhibit higher catalytic performance in biodiesel production. This is attributed to the presence of acidic functional groups, such as —COOH and —OH, which facilitate stronger covalent bonding with —SO_3H groups. These oxygen-containing functional groups are associated with the *D*3 Raman band, also known as the Valley band, which appears more intense in hydrochars compared to their biochar counterparts.

Published research highlights the significance of Raman characteristics in determining the catalytic performance of carbon-based chars. Graphitization (I_D/I_G) reduces their susceptibility to water adsorption during esterification, while the presence of heteroatom-containing functional groups - particularly oxygen-related species associated with the Valley band - facilitates covalent bonding with sulfonic groups, which serve as active catalytic centers. These two properties are inherently antagonistic and warrant further investigation.

Recently, Dias et al.[101] synthesized Fe-modified hydrochars that exhibited both relatively high graphitization and Valley band intensities. These materials demonstrated exceptional catalytic performance in the esterification of oleic acid with methanol, achieving efficiency comparable to that of sulfuric acid.

3.6 Infrared spectroscopy

Infrared spectroscopy is frequently used for the characterization of biochar and hydrochar. Spectra are preferably acquired using attenuated total reflectance (ATR), which provides information on the surface functional groups, typically more abundant in hydrochars. The most common FTIR bands observed in biochar and hydrochar are listed in Table 5. FTIR spectra are particularly useful for evaluating the influence of preparation conditions on the properties of these carbon materials.

Keiluweit et al.[102] used FTIR spectral features to evaluate the onset temperatures of key processes during biomass charring. The authors noted that in the 100–200 °C temperature range, no significant changes are observed in the FTIR spectra, as lignocellulosic materials begin to dehydrate only around 300 °C. This dehydration is evidenced by a decrease in the intensity of the broad band in the 3500–3200 cm^{-1} region, associated with —OH stretching vibrations. Thermal decomposition of lignocellulosics begins around 400 °C, leading to the emergence of several new bands in the 1600–1700 cm^{-1} range, corresponding to aromatic —C=C— stretching. At charring temperatures above 500 °C, the intensity of these bands decreases, while bands in the 885–752 cm^{-1} region - indicative of polycyclic aromatic hydrocarbons (PAHs) - increase, reflecting the development of condensed aromatic structures.

Saha et al.[103] analyzed the FTIR spectra of hydrochar produced by hydrothermal carbonization of pure cellulose and wood to assess the abundance of surface functional groups with acidic character. They quantified these groups by calculating the relative areas of the corresponding IR bands (Fig. 18). The au-

thors concluded that the total amount of acidic surface functional groups increased with HTC temperature, and that the complex composition of wood played a crucial role in their formation.

Additionally, functional groups introduced during synthesis or post-treatment processes can also be identified through FTIR. Dias et al.[27] and Spataru et al.[78] reported the characterization of sulfonic groups in hydrochars catalysts derived from sugars and glycerin. Spectra in Fig. 19 shows the prominent IR features of sulphonated species with $-SO_3H$ features in the range 1023–1025 cm^{-1} and 1139–1218 cm^{-1} and $-C=S$ centered around 1366 cm^{-1}. The infrared spectral characteristics of sulfur-containing functional groups as described above have also been reported by Macawile et al.[106].

Comparing the spectra of fresh hydrochars with those obtained after catalyzing esterification reactions allowed the authors to infer the stability of sulfonic groups under reaction conditions. These groups act as active sites of the catalyst, highlighting the relevance of FTIR in the catalytic characterization of carbon materials. FTIR spectra of biochars after the adsorption of pollutants from wastewater such dyes[14,107] can be used to elucidate the dominant adsorption mechanisms, which is critical for optimizing the preparation conditions of biochars for adsorption applications.

Recently, McCall et al.[108] applied machine learning models to predict biochar stability, in soil, based on FTIR spectra. Among the models tested, the Random Forest (RF) algorithm achieved the highest accuracy, revealing that biochar stability is positively associated with aromaticity and inversely correlated with FTIR features attributed to C—O functional groups.

Inorganic components, ashes from biomass, in biochar and hydrochar, such as carbonates, silicates, phosphates, and sulfates, can complicate the interpretation of FTIR bands. Inorganic compounds are more commonly retained in biochar than in hydrochar, as the high-pressure, aqueous environment of hydrothermal carbonization (HTC) promotes their dissolution and partitioning into the liquid phase[109]. Mineral exhibit bands (Table 6) that often overlap with those of organic functional groups in char, particularly in the 1000–1200 cm^{-1} region, where both silicate- and phosphate-related vibrations as well as C—O and C—O—C stretching bands commonly appear[110]. This overlap can obscure or distort signals from important oxygenated groups like carboxyl's and phenols, making it difficult to accurately assess the development of surface chemistry and aromaticity during thermal treatment[111]. Additionally, a high ash content can cause baseline distortions and introduce —OH stretching bands related to hydration, further hiding key organic features.

3.7 Thermogravimetry

Thermogravimetric analysis is used to evaluate

Table 5 FTIR bands of biochar and hydrochar attribution (data from literature[105])

Band position/cm^{-1}	Vibration modes attribution
3600-3200	—OH stretching vibrations are more intense for hydrochar because the higher temperatures in biochar production in dry atmosphere promote dehydration of the raw biomass. Furthermore, the resulting graphitized biochar is hydrophobic and therefore does not adsorb moisture.
2970–2851	—CH stretching vibrations from aliphatic groups ($-CH_2$, $-CH_3$). These bands are often more intense in hydrochar compared to biochar, indicating a less carbonized structure.
1701	A prominent band corresponding to —C=O stretching from carboxylic acids, esters, and ketones. This is a key feature of hydrochar and is often less pronounced or absent in high-temperature biochar.
1616	Attributed to —C=C— stretching vibrations of aromatic rings and —C=O stretching in conjugated ketones and quinones.
1459	—CH deformation in lignin and carbohydrates.
1318–1205	—C—O stretching from alcohols, carboxylic acids, esters, and ethers.
1161	A band associated with —C—O—C— from non-charred cellulose.
1060–1030	—C—O stretching from- alcohols and alkyl-substituted ethers.
900-700	PAH vibrations. More pronounced for biochar since hydrochar present lower aromaticity. Specific bands: the exact position of these bands depends on the substitution pattern of the aromatic rings (i.e., how many C—H bonds are on the ring). 900–860 cm^{-1}: Out-of-plane bending for isolated aromatic C—H. 860–800 cm^{-1}: Out-of-plane bending for two adjacent C-H bonds on a ring. 800–750 cm^{-1}: Out-of-plane bending for three or four adjacent C-H bonds. 750–700 cm^{-1}: Out-of-plane bending for five adjacent C—H bonds.

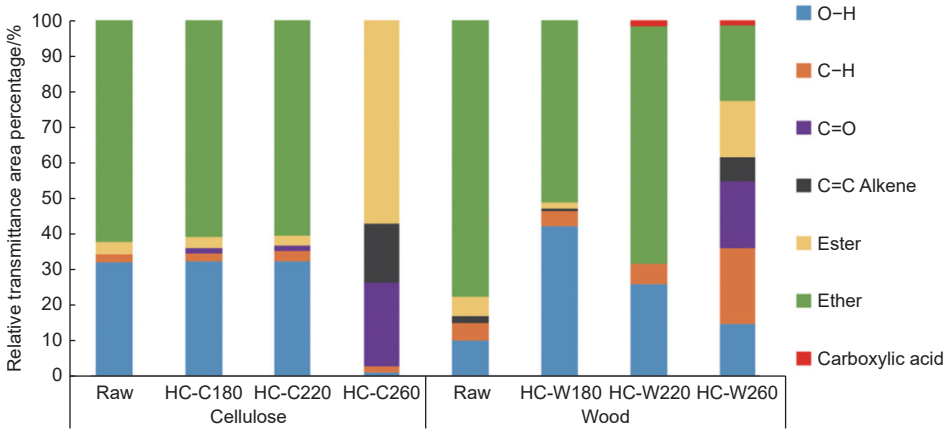

Fig. 18 Relative abundance of surface functional groups in hydrochars produced at various pyrolysis temperatures, as determined by FTIR spectroscopy. Spectra of the corresponding raw biomasses are included for comparison (Reproduced from[104], copyright 2019, with Elsevier permission)

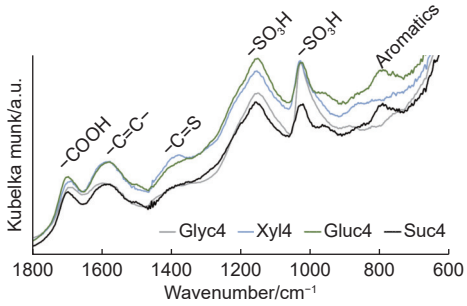

Fig. 19 FTIR spectra of sugar (xylose, glucose and sucrose) and glycerin derived hydrochar obtained by HTC with simultaneous sulphonation (Reproduced from[78], copyright 2021, with Elsevier permission)

the structural stability of biochar and hydrochar by tracking weight loss as the material is subjected to a controlled heating rate under specific atmospheric conditions. Tests conducted in a nitrogen (N_2) or air environment revealed distinct differences between biochar and hydrochar, indicating that both the production method and the type of feedstock influence the thermal decomposition behavior of these materials.

According to E. Taskin et al., under a N_2 atmosphere, the volatilization and decomposition intervals of the biochar and hydrochar samples could not be distinctly identified. Under inert conditions, hydrochar exhibited a markedly higher degree of thermal degradation with increasing temperature compared to biochar[117]. The thermogravimetric curves of biochar samples remained nearly horizontal, indicative of minimal mass loss. In contrast, total weight loss under N_2 reached up to 18% for biochars and up to 76% for hydrochars. These results underscore the significant influence of production methods on thermal stability under inert atmospheres, with biochars displaying substantially greater resistance to thermal decomposition. The enhanced stability of biochar is primarily attributed to its higher lignin content, whereas hydrochar, characterized by elevated levels of cellulose and hemicellulose, demonstrated greater thermal instability. They demonstrated that hydrochars exhibited significantly greater carbon loss under a N_2 atmosphere indicating lower thermal stability[117].

Soares Dias et al. investigated the thermal stability of the synthesized hydrochars using thermogravimetric analysis under a nitrogen atmosphere. The mass loss behavior of the produced hydrochars was not clearly defined, likely due to the considerable variability of biomass types and the differing methods and conditions employed for char production. Overall,

Table 6 FTIR bands of inorganics in biochar and hydrochar

Inorganic	Wavenumber/(cm^{-1})	Vibrational mode	Refs.
Carbonates (e.g., $CaCO_3$)	1400–1450; 875; 710	Asymmetric/symmetric C—O stretching and bending	[112]
Phosphates (e.g., $Ca_3(PO_4)_2$)	1100–1000; 600–560	PO_4^{3-} asymmetric stretching and bending	[113]
Silicates (e.g., SiO_2)	1100–1000; 470	Si—O—Si asymmetric stretching and bending	[114]
Sulfates (e.g., $CaSO_4$)	1120–1100; 670–600	SO_4^{2-} stretching and bending	[115]
Metal oxides (e.g., Fe_2O_3, Al_2O_3)	<600	M—O stretching modes (often weak or overlapping)	[116]

mass losses ranged from 60% to 80%. All samples exhibited a process with a maximum mass loss rate within the 150–200 °C range, which appears to correspond to the combined effects of moisture evaporation and the degradation of low molecular weight compounds[27]. Recent data from the same laboratory[101] compared the thermal stability of hydrochar produced from corn starch with that of a commercial petroleum-derived biochar (Aldrich). As shown in Fig. 20, thermogravimetric analysis (TGA) indicates that the hydrochar exhibits a substantially lower thermal degradation onset temperature than the commercial biochar, which maintains stability up to approximately 500 °C. This higher stability is consistent with the greater degree of graphitization, and typical lower oxygen content[6], of the commercial biochar. Furthermore, analysis of the hydrochar after undergoing oleic acid methanolysis showed an increase in thermal stability, attributed to the selective dissolution of the less graphitized fractions by the reaction medium. This finding suggests the formed esters appear to be effective in removing amorphous carbon fractions from the material.

Under an air atmosphere, hydrochars showed substantially lower carbon loss compared to biochars within the 400–700 °C range. However, between 500–900 °C, the carbon loss of hydrochars exceeded that of biochars. This behavior suggests a higher proportion of thermally stable constituents in hydrochars, such as inorganic residues and char[117]. Xu et al. found that hydrochars exhibited different weight loss patterns at various stages compared to biochars. Hydrochar combustion occurred at lower temperatures, indicating their lower thermal stability[118]. Thermogravimetry also makes it possible to calculate kinetic parameters (in particular, the activation energy and the pre-exponential factor) from thermogravimetric experimental data obtained at different heating rates and to estimate the composition of the sample by deconvoluting the experimental DTG curve using symmetrical Gaussian functions[119–121]. This method assumes that each component degrades independently, with the total DTG curve being the sum of the individual curves. The key parameters - amplitude, position and width - were optimized to fit the curve. The deconvolution identified the main components of the biomass, such as moisture, hemicellulose, cellulose and lignin, consistent with the known compositions of similar types of biomass[119–121]. This deconvolution method can also be applied to identify the main components of chars that are being degraded, such as moisture, volatiles still present and even traces of remaining lignin.

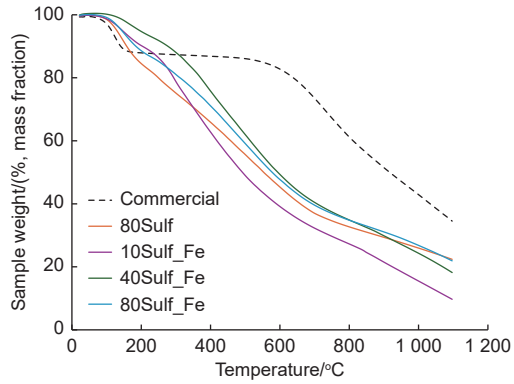

Fig. 20 Comparison of the thermal stability of the hydrochars produced with Aldrich's commercial char, used as a reference (Reproduced from[101])

3.8 Boehm titration

The Boehm titration differentiates acidic functional groups based on their reactivity with bases of varying strengths. NaOH deprotonates all Brønsted acids and hydrolyzes lactones/lactols; Na_2CO_3 targets acids with pKa < 10.3; and $NaHCO_3$ reacts with acids with pKa < 6.4. These allow for quantitative estimation of functional groups across defined pKa ranges. Accurate results depend on complete CO_2 removal and retention of functional groups in the solid phase. The method has recently been standardized for carbon blacks, with key improvements in endpoint detection, titrant strength, and filtration procedures.

Although originally developed for carbon blacks and activated carbons, the Boehm titration has been increasingly applied to biochars. However, differences such as higher carbon solubility and ash content in biochars may compromise its accuracy[122]. Fidel et al. evaluated 3 carbonate and dissolved organic compounds (DOC) removal methods (sparging, barium chloride treatment, and solid-phase extraction) for their effectiveness in improving Boehm titration

reliability[122]. Results showed that no method was entirely free of bias across all pKa ranges, with the cartridge method consistently biased. The most reliable combination was the sparge method for low pKa groups (~ 5–6.4) and the barium method for higher pKa groups (~ 6.4–13). Nevertheless, according to Fidel et al., further validation is needed, and Boehm titration results for biochars should be treated with caution unless appropriate interference removal steps are taken[122].

Rani et al. investigated rice straw-derived hydrochar (RSH) and its carboxylate-functionalized form (RSHC) as adsorbents, where RSHC was produced by selectively converting phenolic oxygen-containing groups on the RSH surface into carboxylate functionalities, thereby enhancing the density of carboxylate groups[123]. The modification of RSH to RSHC which resulted in an increase in pH to 9.5, indicating effective neutralization of acidic functional groups. Boehm titration confirmed these modifications, showing the complete removal of phenolic groups and an increase in lactone functionalities. Based on this method, Rani et al. concluded that phenolic groups were fully substituted, likely forming carboxylate derivatives that underwent cyclization under basic conditions[123].

Saha et al. prepared hydrochars from cellulose and wood using hydrothermal carbonization (HTC) at 180, 220 and 260 °C, with a residence time of 30 min[104]. To assess the surface acidity and the presence of oxygen-containing functional groups, they applied Boehm titration, which allowed for quantifying the concentration and dissociation behavior of acidic sites on the hydrochar surfaces. In raw cellulose, no lactonic groups were detected, which is consistent with its structure as a linear polymer of D-glucose units linked by $\beta(1\rightarrow4)$ glycosidic bonds[104]. Phenolic and carboxylic group concentrations were measured at 7.4 and 13.1 μmol/g, respectively. After treatment at 180 °C, there was little change in surface chemistry. However, heating the cellulose to 220 °C led to a significant increase in all 3 types of acidic functional groups. At this temperature, carboxylic, lactonic, and phenolic groups were present at 33.6, 21.0 and 63.4 μmol g^{-1}, respectively, suggesting that HTC at elevated temperatures enhances the chemical functionality of the hydrochar surface[104].

4 Conclusions

Biochar and hydrochar are 2 distinct, carbon-rich materials produced from biomass by pyrolysis and hydrothermal carbonization (HTC), respectively. The fundamental differences in their production pathways lead to materials with widely varying physicochemical properties. Biochar is characterized by high porosity, large surface area, high aromaticity and superior thermal stability (making it excellent for long-term CO_2 sequestration and gas-phase applications). In contrast, hydrochar features a denser, less porous structure, higher oxygen content, and an abundance of surface functional groups (like carboxyl, hydroxyl and carbonyl groups), which lend themselves well to aqueous-phase reactions and liquid adsorption. Comprehensive characterization by techniques such as BET, SEM, XPS, XRD, and Raman spectroscopy has been crucial for linking these structural and chemical attributes to their performance, confirming the potential of both materials to address diverse environmental and technological challenges.

The future of carbon-rich materials lies in targeted design and enhanced deployment, requiring focus on the following key areas:

(1) Application-driven material design: moving beyond simple material production to the rational design of chars tailored for specific functions (e.g., enhanced CO_2 adsorption capacity, selective catalytic activity, or optimized pollutant removal). This includes advanced post-treatment and functionalization methods.

(2) Integration of advanced analytics: implementing and integrating sophisticated techniques like in situ characterization during production or reaction and Machine Learning algorithms to predict material performance based on feedstock and production parameters. This will accelerate the development cycle and optimize properties efficiently.

(3) Sustainable and scalable industrial deployment: overcoming economic and logistical hurdles to facilitate the industrial-scale production and use of biochar and hydrochar. This requires developing robust, energy-efficient production systems and securing supply chains for diverse feedstocks.

(4) Novel and integrated system applications: exploring their role in integrated biorefinery concepts (utilizing all output fractions), resource recovery (e.g., phosphorus from wastewater), and next-generation energy storage/conversion systems, further leveraging their unique surface chemistry and structural stability.

Authors' contributions

Both authors contributed equally to the conception, literature review, and writing of the manuscript. All authors have read and approved the final version.

Acknowledgements

The authors gratefully acknowledge the support of the CERENA (FCT-UIDB/04028/2025 and FCT-UIDP/04028/2025) and VALORIZA – Research Centre for Endogenous Resource Valorization (FCT-UID/05064/2025).

References

[1] Shoudho K N, Khan T H, Ara U R, et al. Biochar in global carbon cycle: Towards sustainable development goals[J]. Current Research in Green and Sustainable Chemistry, 2024, 8: 100409.

[2] Padhye L P, Bandala E R, Wijesiri B, et al. Hydrochar: A promising step towards achieving a circular economy and sustainable development goals[J]. Frontiers in Chemical Engineering, 2022, 4: 867228.

[3] Kumar A, Saini K, Bhaskar T. Hydochar and biochar: Production, physicochemical properties and techno-economic analysis[J]. Bioresource Technology, 2020, 310: 123442.

[4] Biochar Market Size Is Expanding Around USD 3, 111.96 Mn By 2034[EB/OL].[2025-07-31]. https://www.precedenceresearch.com/biochar-market.

[5] Kambo H S, Dutta A. A comparative review of biochar and hydrochar in terms of production, physico-chemical properties and applications[J]. Renewable and Sustainable Energy Reviews, 2015, 45: 359-378.

[6] Ercan B, Alper K, Ucar S, et al. Comparative studies of hydrochars and biochars produced from lignocellulosic biomass via hydrothermal carbonization, torrefaction and pyrolysis[J]. Journal of the Energy Institute, 2023, 109: 101298.

[7] Cognigni P, Leonelli C, Berrettoni M. A bibliographic study of biochar and hydrochar: Differences and similarities[J]. Journal of Analytical and Applied Pyrolysis, 2025, 187: 106985.

[8] Atkinson C J, Fitzgerald J D, Hipps N A. Potential mechanisms for achieving agricultural benefits from biochar application to temperate soils: A review[J]. Plant and Soil, 2010, 337(1): 1-18.

[9] Kozioł A, Paliwoda D, Mikiciuk G, et al. Biochar as a multi-action substance used to improve soil properties in horticultural and agricultural crops—a review[J]. Agriculture, 2024, 14(12): 2165.

[10] Wang L, Chen D, Zhu L. Biochar carbon sequestration potential rectification in soils: Synthesis effects of biochar on soil CO_2, CH_4 and N_2O emissions[J]. Science of The Total Environment, 2023, 904: 167047.

[11] Liu Z, Wang Z, Chen H, et al. Hydrochar and pyrochar for sorption of pollutants in wastewater and exhaust gas: A critical review[J]. Environmental Pollution, 2021, 268: 115910.

[12] Phiri Z, Moja N T, Nkambule T T I, et al. Utilization of biochar for remediation of heavy metals in aqueous environments: A review and bibliometric analysis[J]. Heliyon, 2024, 10(4): e25785.

[13] Khanzada A K, Al-Hazmi H E, Kurniawan T A, et al. Hydrochar as a bio-based adsorbent for heavy metals removal: A review of production processes, adsorption mechanisms, kinetic models, regeneration and reusability[J]. Science of The Total Environment, 2024, 945: 173972.

[14] Soares Dias A P, Santos F A, Rijo B, et al. Seaweed-derived biochar for effective treatment of dye-contaminated wastewater[J]. Water, 2025, 17(8): 1215.

[15] Chauhan S, Shafi T, Dubey B K, et al. Biochar-mediated removal of pharmaceutical compounds from aqueous matrices via adsorption[J]. Waste Disposal & Sustainable Energy, 2022, 5(1): 37-62.

[16] Karki B K. Amended biochar in constructed wetlands: Roles, challenges, and future directions removing pharmaceuticals and personal care products[J]. Heliyon, 2024, 10(21): e39848.

[17] Haider F U, Wang X, Zulfiqar U, et al. Biochar application for remediation of organic toxic pollutants in contaminated soils; An update[J]. Ecotoxicology and Environmental Safety, 2022, 248: 114322.

[18] Ambaye T G, Vaccari M, Van Hullebusch E D, et al. Mechanisms and adsorption capacities of biochar for the removal of organic and inorganic pollutants from industrial wastewater[J]. International Journal of Environmental Science and Technology, 2021, 18(3): 3273-3294.

[19] De Souza T F, Dias Ferreira G M. Biochars as adsorbents of pesticides: Laboratory-scale performances and real-world contexts, challenges, and prospects[J]. ACS ES and T Water, 2024, 4(10): 4264-4282.

[20] Mota L S O, de oliveira P C O, Peixoto B S, et al. Biochar applications in microplastic and nanoplastic removal: mechanisms and integrated approaches[J]. Environmental Science: Water Research & Technology, 2025, 11(2): 222-241.

[21] Chen L, Fang W, Liang J, et al. Biochar application in anaerobic digestion: Performances, mechanisms, environmental assessment and circular economy[J]. Resources, Conservation and Recycling, 2023, 188: 106720.

[22] Zhao L, Xiao D, Liu Y, et al. Biochar as simultaneous shelter, adsorbent, pH buffer, and substrate of Pseudomonas citronellolis to promote biodegradation of high concentrations of phenol in wastewater[J]. Water Research, 2020, 172: 115494.

[23] Jiang T, Wang B, Gao B, et al. Degradation of organic pollutants from water by biochar-assisted advanced oxidation processes: Mechanisms and applications[J]. Journal of Hazardous Materials, 2023, 442: 130075.

[24] Gasim M F, Lim J W, Low S C, et al. Can biochar and hydrochar be used as sustainable catalyst for persulfate activation?[J]. Chemosphere, 2022, 287: 132458.

[25] Cui J, Zhang F, Li H, et al. Recent progress in biochar-based photocatalysts for wastewater treatment: synthesis, mechanisms, and applications[J]. Applied Sciences, 2020, 10(3): 1019.

[26] Xiong X, Yu I K M, Cao L, et al. A review of biochar-based catalysts for chemical synthesis, biofuel production, and pollution control[J]. Bioresource Technology, 2017, 246: 254-270.

[27] Paula Soares Dias A, Saraiva N, Rijo B, et al. Sugar derived hydrochar catalysts for enhanced biodiesel production via esterification[J]. Fuel, 2024, 374: 132459.

[28] Soares Dias A P, Pedra I, Salvador É, et al. Biodiesel production over banana peel biochar as a sustainable catalyst[J]. Catalysts, 2024, 14(4): 266.

[29] Yadav G, Yadav N, Ahmaruzzaman M. Advances in biomass derived low-cost carbon catalyst for biodiesel production: preparation methods, reaction conditions, and mechanisms[J]. RSC Advances, 2023, 13(33): 23197-23210.

[30] Man K Y, Chow K L, Man Y B, et al. Use of biochar as feed supplements for animal farming[J]. Critical Reviews in Environmental Science and Technology, 2021, 51(2): 187-217.

[31] Akbari A, Peighambardoust S J, Kazemian H. Comparative study on the impact of physicochemical characteristics of the activated carbons derived from biochar/hydrochar on the adsorption performances[J]. Environmental Research, 2025, 270: 121022.

[32] Dieguez-Alonso A, Funke A, Anca-Couce A, et al. Towards biochar and hydrochar engineering —influence of process conditions on surface physical and chemical properties, thermal stability, nutrient availability, toxicity and wettability[J]. Energies, 2018, 11(3): 496.

[33] Shafawi A N, Mohamed A R, Lahijani P, et al. Recent advances in developing engineered biochar for CO_2 capture: An insight into the biochar modification approaches[J]. Journal of Environmental Chemical Engineering, 2021, 9(6): 106869.

[34] Faggiano A, Cicatelli A, Guarino F, et al. Optimizing CO_2 capture: Effects of chemical functionalization on woodchip biochar adsorption performance[J]. Journal of Environmental Management, 2025, 380: 125059.

[35] Wen C, Liu T, Wang D, et al. Biochar as the effective adsorbent to combustion gaseous pollutants: Preparation, activation, functionalization and the adsorption mechanisms[J]. Progress in Energy and Combustion Science, 2023, 99: 101098.

[36] Jia W, Li S, Wang J, et al. Sustainable valorisation of food waste into engineered biochars for CO_2 capture towards a circular economy[J].Green Chemistry, 2024,26, 1790-1805.

[37] Pandit C, Wang C T, Ong H C. Potential mechanisms and application of biochar in electrochemical systems[J]. Applied Energy, 2025, 397: 126351.

[38] Chen W, Shi X, Peng Y, et al. Biomass pyrolysis for N-doped biochar: Relationship among preparation process, N-doped biochar properties, and supercapacitors[J]. Fuel, 2026, 404: 136372.

[39] Xue C F, Lin Y, Zhao W, et al. Green preparation of high active biochar with tetra-heteroatom self-doped surface for aqueous electrochemical supercapacitor with boosted energy density[J]. Journal of Energy Storage, 2024, 90: 111872.

[40] Makinde W O, Hassan M A, Pan Y, et al. Sulfur and nitrogen co-doping of peanut shell-derived biochar for sustainable supercapacitor applications[J]. Journal of Alloys and Compounds, 2024, 991: 174452.

[41] Bartoli M, Piovano A, Elia G A, et al. Pristine and engineered biochar as Na-ion batteries anode material: A comprehensive overview[J]. Renewable and Sustainable Energy Reviews, 2024, 194: 114304.

[42] Seroka N S, Luo H, Khotseng L. Biochar-derived anode materials for lithium-ion batteries: A review[J]. Batteries, 2024, 10(5): 144.

[43] Zhu L, Zhang W, Chen J, et al. Deciphering the storage mechanism of biochar anchored with different morphology Mn_3O_4 as advanced anode material for lithium-ion batteries[J]. Journal of Colloid and Interface Science, 2024, 669: 740-753.

[44] Patwardhan S B, Pandit S, Kumar Gupta P, et al. Recent advances in the application of biochar in microbial electrochemical cells[J]. Fuel, 2022, 311: 122501.

[45] Li D, Zheng Y, Sun Y, et al. Biochar for electrochemical treatment of wastewater[J]. Biochar Applications for Wastewater Treatment, 2023: 171-192.

[46] He L, Wei S, Zhang X, et al. Research progress on high-rate graphite anode materials for lithium-ion batteries[J]. Journal of Energy Storage, 2025, 111: 115426.

[47] Lobato-Peralta D R, Okoye P U, Alegre C. A review on carbon materials for electrochemical energy storage applications: State of the art, implementation, and synergy with metallic compounds for supercapacitor and battery electrodes[J]. Journal of Power Sources, 2024, 617: 235140.

[48] Wu F, Zhao Y, Hou Z, et al. Lignocellulosic oxidation bridging to modulate pseudographitic domain of hard carbon toward boosted sodium storage[J]. Journal of Energy Storage, 2025, 130: 117496.

[49] Hou Z, Zhao Y, Du Y, et al. Expediting sodium energy of hard

carbon by cation/anion Co-interfering chemistry[J]. Advanced Functional Materials, 2025, 35(36): 2505468.

[50] Masoumi S, Borugadda V B, Nanda S, et al. Hydrochar: A review on its production technologies and applications[J]. Catalysts, 2021, 11(8): 939.

[51] Do P T, Nguyen L X. A review of thermochemical decomposition techniques for biochar production[J]. Environment, Development and Sustainability, 2024, 2024: 1-57.

[52] Toda M, Takagaki A, Okamura M, et al. Biodiesel made with sugar catalyst[J]. Nature, 2005, 438: 178.

[53] Muzyka R, Misztal E, Hrabak J, et al. Various biomass pyrolysis conditions influence the porosity and pore size distribution of biochar[J]. Energy, 2023, 263: 126128.

[54] White R J, Budarin V, Luque R, et al. Tuneable porous carbonaceous materials from renewable resources[J]. Chemical Society Reviews, 2009, 38(12): 3401-3418.

[55] Wang L, Olsen M N P, Moni C, et al. Comparison of properties of biochar produced from different types of lignocellulosic biomass by slow pyrolysis at 600 °C[J]. Applications in Energy and Combustion Science, 2022, 12: 100090.

[56] Handiso B, Pääkkönen T, Wilson B P. Effect of pyrolysis temperature on the physical and chemical characteristics of pine wood biochar[J]. Waste Management Bulletin, 2024, 2(4): 281-287.

[57] Lee J, Kim K H, Kwon E E. Biochar as a catalyst[J]. Renewable and Sustainable Energy Reviews, 2017, 77: 70-79.

[58] Tomczyk A, Sokołowska Z, Boguta P. Biochar Physicochemical Properties: Pyrolysis Temperature and Feedstock Kind Effects[M]. Reviews in Environmental Science and Biotechnology Springer, 2020: 191-215.

[59] Jia Y, Shi S, Liu J, et al. Study of the effect of pyrolysis temperature on the Cd^{2+} adsorption characteristics of biochar[J]. Applied Sciences , 2018, 8(7): 1019.

[60] Agrafioti E, Bouras G, Kalderis D, et al. Biochar production by sewage sludge pyrolysis[J]. Journal of Analytical and Applied Pyrolysis, 2013, 101: 72-78.

[61] Racek J, Sevcik J, Chorazy T, et al. Biochar – recovery material from pyrolysis of sewage sludge: A review[J]. Waste and Biomass Valorization, 2020, 11(7): 3677-3709.

[62] Thunshirn P, Wenzel W W, Pfeifer C. Pore characteristics of hydrochars and their role as a vector for soil bacteria: A critical review of engineering options[J]. Critical Reviews in Environmental Science and Technology, 2022, 52(23): 4147-4171.

[63] Liu Z, Niu W, Chu H, et al. Temperature for biochar[R]//BioResources: 13. 2018.

[64] Vijayaraghavan K, Balasubramanian R. Application of pinewood waste-derived biochar for the removal of nitrate and phosphate from single and binary solutions[J]. Chemosphere, 2021, 278: 130361.

[65] Chatterjee R, Sajjadi B, Chen W Y, et al. Effect of pyrolysis temperature on physico chemical properties and acoustic-based amination of biochar for efficient CO_2 adsorption[J]. Frontiers in Energy Research, 2020, 8: 530643.

[66] Li W, Yang K, Peng J, et al. Effects of carbonization temperatures on characteristics of porosity in coconut shell chars and activated carbons derived from carbonized coconut shell chars[J]. Industrial Crops and Products, 2008, 28(2): 190-198.

[67] Antonangelo J A, Zhang H, Sun X, et al. Physicochemical properties and morphology of biochars as affected by feedstock sources and pyrolysis temperatures[J]. Biochar, 2019, 1(3): 325-336.

[68] Zhao C, Xu Q, Gu Y, et al. Review of advances in the utilization of biochar-derived catalysts for biodiesel production[J]. ACS Omega, 2023, 8(9): 8190-8200.

[69] Cui H M, Liu Y, Bian J, et al. Catalytic hydrothermal carbonization of corn and rice straws with citric acid: Implications for charcoal production and combustion performance[J]. Industrial Crops and Products, 2024, 219: 119162.

[70] Ledesma B, Olivares-Marín M, Álvarez-Murillo A, et al. Method for promoting in-situ hydrochar porosity in hydrothermal carbonization of almond shells with air activation[J]. Journal of Supercritical Fluids, 2018, 138: 187-192.

[71] Nizamuddin S, Mubarak N M, Tiripathi M, et al. Chemical, dielectric and structural characterization of optimized hydrochar produced from hydrothermal carbonization of palm shell[J]. Fuel, 2016, 163: 88-97.

[72] Shao Y, Tan H, Shen D, et al. Synthesis of improved hydrochar by microwave hydrothermal carbonization of green waste[J]. Fuel, 2020, 266: 117146.

[73] Leng L, Xiong Q, Yang L, et al. An Overview on Engineering the Surface Area and Porosity of Biochar[M]//Science of the Total Environment, Elsevier, 2021.

[74] Premchand P, Demichelis F, Galletti C, et al. Enhancing biochar production: A technical analysis of the combined influence of chemical activation (KOH and NaOH) and pyrolysis atmospheres (N_2/CO_2) on yields and properties of rice husk-derived biochar[J]. Journal of Environmental Management, 2024, 370, 123034, 123034.

[75] Munzeiwa W A, Tsekoa P, Kammies L R D, et al. Influence of biomass baseline potential on biochar properties and performance for targeted applications[J]. Discover Water, 2025, 5: 77.

[76] Härmas M, Thomberg T, Romann T, et al. Carbon for energy storage derived from granulated white sugar by hydrothermal carbonization and subsequent zinc chloride activation[J]. Journal of The Electrochemical Society, 2017, 164(9): A1866-A1872.

[77] Zhao H, Zhong H, Jiang Y, et al. Porous $ZnCl_2$-activated carbon from shaddock peel: Methylene blue sdsorption behavior[J]. Materials, 2022, 15(3): 895.

[78] Spataru D, Soares Dias A P, Vieira Ferreira L F. Acetylation of biodiesel glycerin using glycerin and glucose derived catalysts[J]. Journal of Cleaner Production, 2021, 297: 126686.

[79] Souza M C G, Batista A C F, Cuevas R F, et al. Simultaneous carbonization and sulfonation of microcrystalline cellulose to obtain solid acid catalyst and carbon quantum dots[J]. Bioresource Technology Reports, 2022, 19: 101193.

[80] Cognigni P, Leonelli C, Berrettoni M. A Bibliographic Study of Biochar and Hydrochar: Differences and Similarities[M].Journal

of Analytical and Applied Pyrolysis, Elsevier, 2025.

[81] Ercan B, Alper K, Ucar S, et al. Comparative studies of hydrochars and biochars produced from lignocellulosic biomass via hydrothermal carbonization, torrefaction and pyrolysis[J]. Journal of the Energy Institute, 2023, 109: 101298.

[82] Fu M M, Mo C H, Li H, et al. Comparison of physicochemical properties of biochars and hydrochars produced from food wastes[J]. Journal of Cleaner Production, 2019, 236: 117637.

[83] Kang X, Peng J, Ragauskas A J, et al. Competitive effects of glucan's main hydrolysates on biochar formation: A combined experiment and density functional theory analysis[J]. Bioresource Technology, 2022, 359: 127427.

[84] Li Y, Hagos F M, Chen R, et al. Rice husk hydrochars from metal chloride-assisted hydrothermal carbonization as biosorbents of organics from aqueous solution[J]. Bioresources and Bioprocessing, 2021, 8(1): 99.

[85] Yue F, Zhang J, Pedersen C M, et al. Valorization of furfural residue by hydrothermal carbonization: Processing optimization, chemical and structural characterization[J]. Chemistry Select, 2017, 2(2): 583-590.

[86] Ponce S, Paucar M, Stern M, et al. A comparative study of bamboo biochar and hydrochar for pollutant removal[J]. Chemical Engineering Transactions, 2025, 121: 187-92.

[87] Igalavithana A D, Mandal S, Niazi N K, et al. Advances and future directions of biochar characterization methods and applications[J]. Critical Reviews in Environmental Science and Technology, 2017, 47(23): 2275-2330.

[88] Sajjadi B, Chen W Y, Egiebor N O. A comprehensive review on physical activation of biochar for energy and environmental applications[J]. Reviews in Chemical Engineering, 2019, 35(6): 735-776.

[89] Yip K, Xu M, Li C Z, et al. Biochar as a fuel: 3. mechanistic understanding on biochar thermal annealing at mild temperatures and its effect on biochar reactivity[J]. Energy & Fuels, 2011, 25(1): 406-414.

[90] Divyangkumar N, Panwar N L. Optimizing high performance biochar from sugarcane bagasse and corncob via vacuum pyrolysis[J]. Energy 360, 2025, 3: 100014.

[91] Yildiz G, Ronsse F, Venderbosch R, et al. Effect of biomass ash in catalytic fast pyrolysis of pine wood[J]. Applied Catalysis B: Environmental, 2015: 203-211.

[92] Salvador É. Biodiesel production by oleic acid methanolysis over waste biomass hydrochar catalysts[EB/OL]. (2024)[2025-03-21]. https://comum.rcaap.pt/entities/publication/a7db057f-7626-4398-af0c-5e2045a3305d.

[93] Wen H, Li J, Wang X, et al. Comparative study on combustion characteristics of biomass digestate-derived pyrochar and hydrochar: Insights from structural composition and oxygen-containing groups[J]. Fuel, 2025, 389: 134627.

[94] Shan R, Han J, Gu J, et al. A review of recent developments in catalytic applications of biochar-based materials[J]. Resources, Conservation and Recycling, 2020, 162: 105036.

[95] Yan P, Zhang B, Wu K H, et al. Surface chemistry of nanocarbon: Characterization strategies from the viewpoint of catalysis and energy conversion[J]. Carbon, 2019, 143: 915-936.

[96] Guizani C, Haddad K, Limousy L, et al. New insights on the structural evolution of biomass char upon pyrolysis as revealed by the Raman spectroscopy and elemental analysis[J]. Carbon, 2017, 119: 519-521.

[97] Sevilla M, Fuertes A B. The production of carbon materials by hydrothermal carbonization of cellulose[J]. Carbon, 2009, 47(9): 2281-2289.

[98] Ferrari A, Robertson J. Interpretation of Raman spectra of disordered and amorphous carbon[J]. Physical Review B - Condensed Matter and Materials Physics, 2000, 61(20): 14095-14107.

[99] Clohessy J, Kwapinski W. Carbon-based catalysts for biodiesel production—A review[J]. Applied Sciences, 2020, 10(3): 918.

[100] Stepacheva A A, Markova M E, Lugovoy Y V, et al. Plant-biomass-derived carbon materials as catalyst support, a brief review[J]. Catalysts, 2023, 13(4): 655.

[101] Ana Paula Soares Dias, Érica Salvador, Igor Pedra, et al. Starch hydrochar catalysts[J]. Submitted Waste and Biomass Valorization.

[102] Keiluweit M, Nico P S, Johnson M, et al. Dynamic molecular structure of plant biomass-derived black carbon (biochar)[J]. Environmental Science and Technology, 2010, 44(4): 1247-1253.

[103] Saha N, Mcgaughy K, Reza M T. Elucidating hydrochar morphology and oxygen functionality change with hydrothermal treatment temperature ranging from subcritical to supercritical conditions[J]. Journal of Analytical and Applied Pyrolysis, 2020, 152: 104965.

[104] Saha N, Saba A, Reza M T. Effect of hydrothermal carbonization temperature on pH, dissociation constants, and acidic functional groups on hydrochar from cellulose and wood[J]. Journal of Analytical and Applied Pyrolysis, 2019, 137: 138-145.

[105] Hagner M, Salmela M J, Ahmadi S, et al. Biochar and hydrochar from organic side-streams induce species-specific responses in plants[J]. Journal of Soil Science and Plant Nutrition, 2025: 1-19.

[106] Macawile M C, Quitain A T, Kida T, et al. Green synthesis of sulfonated organosilane functionalized multiwalled carbon nanotubes and its catalytic activity for one-pot conversion of high free fatty acid seed oil to biodiesel[J]. Journal of Cleaner Production, 2020, 275: 123146.

[107] Xie Q Q, Yang X, Xu K N, et al. Conversion of biochar to sulfonated solid acid catalysts for spiramycin hydrolysis: insights into the sulfonation process[J]. Environmental Research, 2020, 188: 109887.

[108] Mccall M A, Watson J S, Tan J S W, et al. Biochar stability revealed by FTIR and machine learning[J]. ACS Sustainable Resource Management, 2025, 2(5): 842-852.

[109] GoktepeII G. Utilization of intrinsic inorganic elements: A novel self-activation approach for hierarchical porous carbons from hydrochars[J]. Biomass and Bioenergy, 2025, 197: 107814.

[110] Li S, Skelly S. Physicochemical properties and applications of biochars derived from municipal solid waste: A review[J]. Environmental Advances, 2023, 13: 100395.

[111] Yin Y, Yin H, Wu Z, et al. Characterization of coals and coal

ashes with high Si content using combined second-derivative infrared spectroscopy and Raman spectroscopy[J]. Crystals, 2019, 9(10): 513.

[112] Chen Y, Zhang R, Gao J, et al. The role of silica in biomass for calcium-modified biochar: Phosphorus removal mechanism and potential as a phosphate fertilizer application[J]. Journal of Environmental Sciences, 2025, 158: 242-253.

[113] Bekiaris G, Peltre C, Jensen L S, et al. Using FTIR-photoacoustic spectroscopy for phosphorus speciation analysis of biochars[J]. Spectrochimica Acta Part A: Molecular and Biomolecular Spectroscopy, 2016, 168: 29-36.

[114] Severo F F, Da Silva L S, Moscôso J S C, et al. Chemical and physical characterization of rice husk biochar and ashes and their iron adsorption capacity[J]. SN Applied Sciences, 2020, 2(7): 1-9.

[115] Kiefer J, Strk A, Kiefer A L, et al. Infrared spectroscopic analysis of the inorganic deposits from water in domestic and technical heat exchangers[J]. Energies, 2018, 11(4): 798.

[116] Li Y, Yin H, Cai Y, et al. Regulating the exposed crystal facets of α-Fe_2O_3 to promote Fe_2O_3-modified biochar performance in heavy metals adsorption[J]. Chemosphere, 2023, 311: 136976.

[117] Taskin E, De Castro Bueno C, Allegretta I, et al. Multianalytical characterization of biochar and hydrochar produced from waste biomasses for environmental and agricultural applications[J]. Chemosphere, 2019, 233: 422-430.

[118] Xu S, Chen J, Peng H, et al. Effect of biomass type and pyrolysis temperature on nitrogen in biochar, and the comparison with hydrochar[J]. Fuel, 2021, 291: 120128.

[119] Rijo B, Soares Dias A P, De Jesus N, et al. Home trash biomass valorization by catalytic pyrolysis[J]. Environments - MDPI, 2023, 10(10): 106535.

[120] Soares Dias A P, Rijo B, Ramos M, et al. Pyrolysis of burnt maritime pine biomass from forest fires[J]. Biomass and Bioenergy, 2022, 163.

[121] Rijo B, Soares Dias A P, Saksiwi N D, et al. Biofuels from pyrolysis of third-generation biomass from household and garden waste composting bin: Kinetics analysis[J]. Reactions, 2023, 4(2): 295-310.

[122] Fidel R B, Laird D A, Thompson M L. Evaluation of modified boehm titration methods for use with biochars[J]. Journal of Environmental Quality, 2013, 42(6): 1771-1778.

[123] Rani A, Rongpipi M, Bhardwaj A, et al. Improved carboxylate density hydrochar by alkylation of surface phenol for adsorption of cationic dye in aqueous solution[J]. Surfaces and Interfaces, 2025, 56: 105511.